Synthesis of D-glucono-1,4-lactones modified with linear saturated fatty acids and evaluation of their physical properties

Shiro Komba*

Institute of Food Research, National Agriculture and Food Research Organization, 2-1-12 Kannondai, Tsukuba, Ibaraki 305-8642, Japan

*Correspondence: skomba@affrc.go.jp; Tel.: +81-29-838-7298

10 **Table of Contents/Abstract Graphics**

11

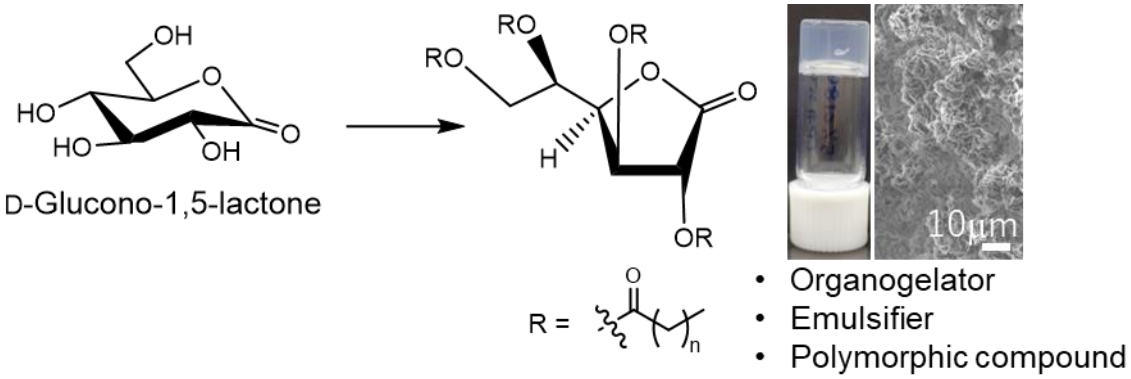

12

Abstract

To develop a novel low molecular–weight organogelator, D-glucono-1,4-lactones, in which all hydroxy groups were esterified with linear saturated fatty acids, were synthesized, and their gelation ability was evaluated. When a fatty acid was introduced, the six-membered ring D-glucono-1,5-lactone changed to a five-membered ring D-glucono-1,4-lactone, regardless of the length of the fatty acid. However, the gelation ability depended on the length of the fatty acid, and compounds esterified with palmitic acid (16 carbons) and stearic acid (18 carbons) showed a better gelation ability. Electron microscopy showed that the structure of the xerogels varied with the length of the fatty acids, with some forming a fiber structure and others forming plate-like crystals building up to a porous structure. In addition, their emulsification ability and crystal polymorphism were confirmed, and detailed polymorphic crystal analysis by FT-IR was performed to estimate the intermolecular packing structure at the molecular level.

Keywords: *D-glucono-1,5-lactone, D-glucono-1,4-lactone, 1,5-GL, 1,4-GL, C16GL, C18GL, organogelator, emulsifier, crystal polymorphism*

1. Introduction

Organogelators include low molecular–weight organogelators (LMG) and polymeric organogelators. LMGs express their functions by creating three-dimensional supramolecular structures, such as self-assembled fibrous structures, through noncovalent bonds, such as van der Waals interactions, π–π interactions, solvophobic effects, and hydrogen bonding. Various sugar derivatives have been developed as LMGs.[1] D-glucose has been the most well studied among the sugars, and various derivatives have been developed as organogelators.[2-6] However, synthesizing various organogelators derived from D-glucose inevitably requires multiple steps. This is because the anomeric position of D-glucose can form two stereoisomers, α- and β-forms, and α-methyl glycosylation is often performed first to fix either one of them.

Various LMGs using D-gluconic acid, the ring-opened structure of D-glucono-1,5-lactone (1,5-GL), have already been developed. Song et al. have reported that D-gluconic acid derivatives with a benzylidene group at the 2,4-position hydroxy groups and an alkylamide group at the 1-position can be used as organogelators.[7, 8] Fang et al. have reported that D-gluconic acid derivatives with a benzylidene group at the 2,4-position hydroxy groups and a methyl ester group at the 1-position can be used as organogelators.[9] These are derivatives of the linear D-gluconic acid and are immobilized with a benzylidene group that can control the molecular mobility of the 2,4-position hydroxy groups. These compounds with such a restrained three-dimensional molecular mobility improve the intermolecular packing ability and facilitate the formation of three-dimensional supramolecular structures, i.e., self-assembled fibrous structures.

Previously, we have developed LMGs in which linear saturated fatty acids are introduced into the hydroxy groups of a six-membered ring cyclic polyol. We have found that 1,5-anhydro-D-glucitol (1,5-AG), one of the six-membered ring cyclic polyols and a compound in which the anomeric position of D-glucose is deoxygenated, is a good organogelator when linear saturated fatty acids are

introduced into all hydroxy groups. Among them, 1,5-anhydro-2,3,4,6-tetra-*O*-hexadecanoyl-D-glucitol (C16AG) (**Figure 1**, compound **8**), which has a 16-carbon palmitic acid, was found to have the best gelation ability.[10-13] Furthermore, it has been found that 1,5-AG derivatives with linear saturated fatty acids containing an amide group can form thinner fibers than those without amide groups, thereby creating stiffer gels.[14] Thus, we retained the six-membered ring structure, which is the sugar backbone, and used this structure to control three-dimensional molecular mobility, thereby improving the packing between molecules and creating a three-dimensional supramolecular structure. Considering practical use, unlike D-glucose, the six-membered ring structure used here is free of stereoisomers, and raw materials that enable the synthesis of the target product in a single step were selected. Applying this idea to 1,5-GL, the six-membered ring structure of D-gluconic acid, and introducing a fatty acid to this hydroxy group, we speculated it would make a good organogelator. 1,5-GL does not have the problem of stereoisomerization at the anomeric position, which has been an issue with D-glucose. Furthermore, unlike 1,5-AG, the oxygen atom of the carbonyl group of the lactone, which has a high electron density, may improve the affinity for water and is expected to develop an emulsifying ability.

Herein, we report the synthesis of gluconolactone derivatives reacted with various linear saturated fatty acids of different lengths and the results of the verification of their gelation and emulsification properties. Furthermore, we also report the discovery of crystal polymorphism as an unexpected physical property of gluconolactone derivatives and the estimation of the molecular packing mechanism at the molecular level based on detailed analysis of the polymorphism.

2. Results and discussion

2.1. Synthesis of gelators

Previous studies have reported on introducing fatty acids to the 6-position hydroxy group of 1,5-GL,[15,

[16] but as far as we know, there are no reports on introducing fatty acids to all hydroxy groups of 1,5-GL. Therefore, we decided to introduce various linear saturated fatty acids of different lengths into 1,5-GL and compare their physical properties. The selected fatty acids were 10-carbon decanoic acid (capric acid), 12-carbon dodecanoic acid (lauric acid), 14-carbon tetradecanoic acid (myristic acid), 16-carbon hexadecanoic acid (palmitic acid), 18-carbon octadecanoic acid (stearic acid), and 22-carbon docosanoic acid (behenic acid), and the acyl chlorides of each were used. However, because there is no commercially available acyl chloride of behenic acid, the acyl chloride was synthesized using thionyl chloride and then used.

1,5-GL was dissolved in 8 equivalents of pyridine and 4 equivalents of 4-dimethylaminopyridine (DMAP). 1,5-GL, being a hydrophilic compound, could dissolve in the pyridine solution containing DMAP. It was then suspended in toluene and reacted by adding 6 equivalents of various fatty acyl chlorides and stirring at room temperature for one day (**Scheme 1**). The compound with capric acid (C10GL) and the compound with behenic acid (C22GL) required purification using silica gel column chromatography, while the other compounds were successfully isolated and purified using crystallizations. The homemade behenoyl chloride was colored, and the color remained after purification of the product, C22GL, by column chromatography. Therefore, the gel during gelation tests was colored.

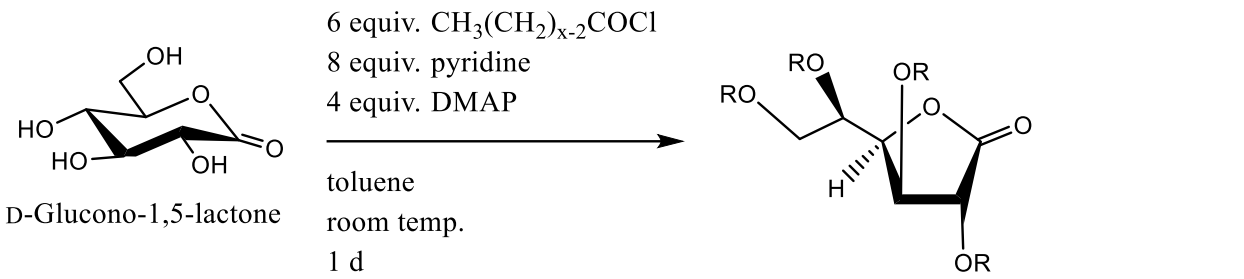

	Compound	X	R	Yield
1	C10GL	10	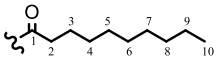	24%[b]
2	C12GL	12	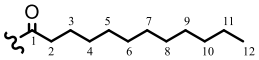	63%[c]
3	C14GL	14	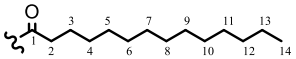	77%[c]
4	C16GL	16	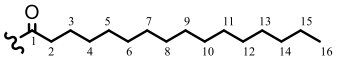	61%[c]
5	C18GL	18	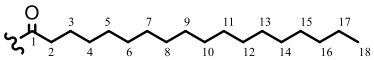	92%[c]
6[a]	C22GL	22	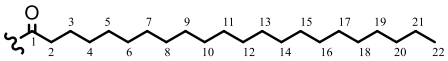	20%[b]

Scheme 1. Introduction of fatty acids of various lengths into 1,5-GL. [a]Since behenoyl chloride is not commercially available, it was synthesized from behenic acid and used without purification. The reaction was conducted at room temperature for one day, followed by 4 h at 80°C. [b]Isolated yield purified using column chromatography. [c]Isolated yield purified using crystallization.

Nuclear magnetic resonance (NMR) analysis of the obtained compounds revealed that they did not have the expected six-membered ring structure with 1,5 cyclization, but all compounds had five-membered ring structures with 1,4 cyclization (D-glucono-1,4-lactone: 1,4-GL). This was confirmed using heteronuclear multiple bond correlation (HMBC)-NMR. Specifically, a cross-peak from the hydrogen at position 4 to the carbon at position 1 and a cross-peak from the hydrogen at position 5 to the carbonyl carbon of the fatty acid were observed for each compound. C10GL (**1**) (δ4.95 (H-4) → 169.04 (C-1), 5.36 (H-5) → 171.93–172.11 (C_{lipid}-1)), C12GL (**2**) (δ4.94 (H-4) → 169.04 (C-1), 5.36 (H-5) → 171.93–172.10 (C_{lipid}-1)), C14GL (**3**) (δ4.94 (H-4) → 169.04 (C-1), 5.36 (H-5) → 171.93–172.10 (C_{lipid}-1)), C16GL (**4**) (δ4.94 (H-4) → 169.04 (C-1), 5.36 (H-5) → 171.93–172.10 (C_{lipid}-1)),

C18GL (**5**) (δ4.94 (H-4) → 169.03 (C-1), 5.36 (H-5) → 171.92–172.10 (C_{lipid}-1)), C22GL (**6**) (δ4.94 (H-4) → 169.03 (C-1), 5.36 (H-5) → 171.92–172.10 (C_{lipid}-1)).

When lauric acid was introduced into the 6-position hydroxy group of 1,5-GL by lipase by Pocalyko et al.,[15] the initial compound synthesized was the one in which the 6-position hydroxy group of 1,5-GL was esterified. This compound decreases with time, and an increase in the compound has been reported in which the 6-position hydroxy group of 1,4-GL, which cyclized at 1,4-position, is esterified. The esterification of the 6-position hydroxy group of 1,5-GL is thought to result in a structural change from a six-membered ring to a five-membered ring, forming 1,4-GL.

Next, fatty acids were selectively introduced to determine which hydroxy groups were least reactive, as well as to investigate the gelation property of a compound in which three of the four hydroxy groups of 1,5-GL have fatty acids and one is a free hydroxy group. We attempted to selectively introduce fatty acids by closely monitoring the reaction with thin-layer chromatography (TLC) and terminating it midway. The fatty acid introduced here was palmitic acid, and the reaction conditions were the same as for the synthesis of C16GL (**4**) except for the reaction time (**Scheme 2**). In a mixture crystallized in acetone, the main compound with a lower Rf value on TLC than fully palmitoylated C16GL (**4**) was purified using silica gel column chromatography, crystallized, and the structure was confirmed using NMR. ^{1}H–^{1}H COSY NMR showed that the hydroxy group at position 5 was free (δ 4.11 (H-5) → 2.75 (OH)), and HMBC-NMR showed that it was a five-membered ring cyclized at 1,4 (δ 4.70 (H-4) → 169.19 (C-1)). Compound **7** (5-OH-C16GL) was confirmed with a free hydroxy group at position 5. This revealed that the hydroxy group at position 5 was the least reactive of the 1,4-GL hydroxy groups.

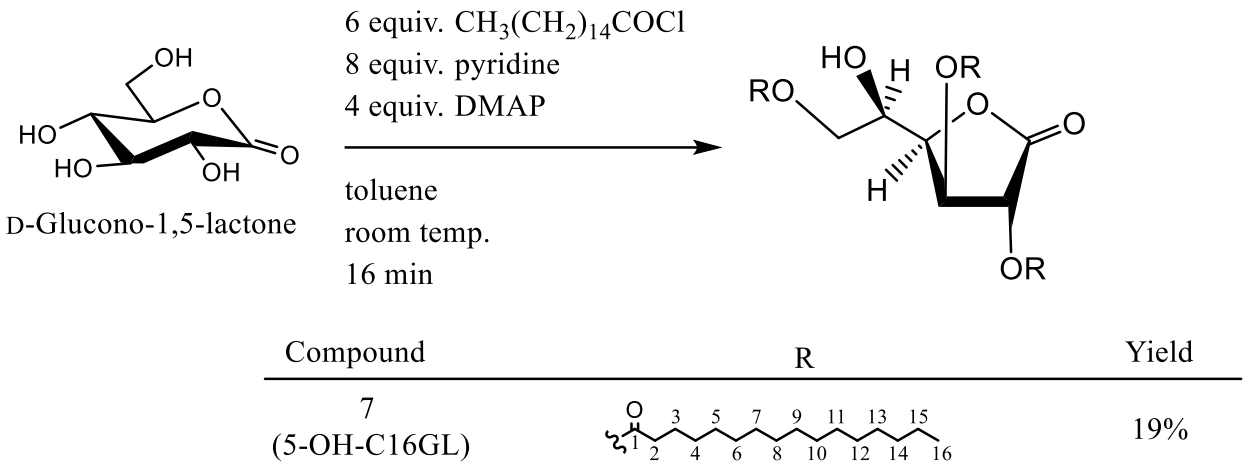

Compound	R	Yield
7 (5-OH-C16GL)		19%

Scheme 2. Selective introduction of palmitic acid.

2.2. Gelation test of each compound

Gelation tests were performed using 2-mL screw-capped glass bottles. Each sample of compounds **2**–**7** (compound **1** was not tested for gelation because it was liquid at room temperature) and C16AG (**8**, **Figure 1**),[10] an existing gelator for comparison, was accurately weighed into these bottles. An accurate amount of liquid paraffin #350 was added to achieve concentrations of 1 wt% and 5 wt%. The mixtures were heated on a hot plate at 100°C–150°C to dissolve the compounds and then left at room temperature for 12 h to form gels. The bottles were inverted; if the content did not flow, it was considered gelated. The gel hardness and relative turbidity were then measured (**Figure 2**, **Table 1**).

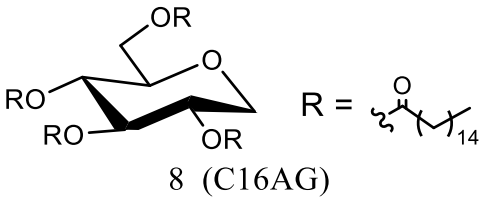

Figure 1. Structure of existing organogelator C16AG (**8**).

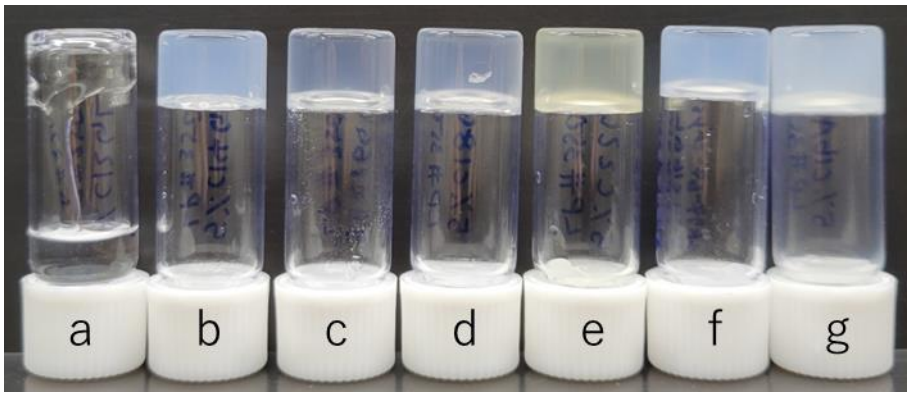

Figure 2. Actual photographs of the formed gels of each sample; 5 wt% gel of each sample in liquid paraffin #350. (a) C12GL (**2**), (b) C14GL (**3**), (c) C16GL (**4**), (d) C18GL (**5**), (e) C22GL (**6**), (f) 5-OH-C16GL (**7**), and (g) C16AG (**8**).

Table 1. Gel hardness and relative turbidity.

	Gel hardness (mN)		Turbidity (660 nm abs. a.u.)
Compound	**1 wt%**	**5 wt%**	**5 wt%**
C12GL (**2**)	-	-	
C14GL (**3**)	-	85	0.56
C16GL (**4**)	8	64	0.13
C18GL (**5**)	2	207	0.20
C22GL (**6**)	-	23	0.50
5-OH-C16GL (**7**)	-	32	0.63
C16AG (**8**)	22	318	1.2

"-" indicates that the compound did not gel and flowed down.

At 1 wt%, only C16GL (**4**) and C18GL (**5**) formed gels, while the others did not. At 5 wt%, all compounds except C12GL (**2**) formed gels. In particular, C18GL (**5**) showed a high gel hardness of 207 mN and relatively low turbidity. Although its hardness was lower than that of C16AG (**8**), an existing gelator, its transparency was higher. 5-OH-C16GL (**7**), which has a free 5-position hydroxy group, had lower gel hardness than the fully palmitoylated C16GL (**4**).

These results indicate an optimal fatty acid chain length for gelation, with 16 and 18 carbons being optimal. The difference between C16GL (**4**) and C16AG (**8**) is the presence or the absence of a carbonyl group at the 1-position and the difference between a five- and six-membered ring. A five-membered ring allows the 5- and 6-position carbons to rotate freely, increasing molecular freedom. Therefore, we speculate that the packing force between molecules is reduced, resulting in lower gel hardness. In addition, a three-dimensional supramolecular structure is necessary for gelation, and C16GL (**4**) and C18GL (**5**) may form thinner or smaller structures owing to their lower turbidity compared with the others. From the comparison of C16GL (**4**) and 5-OH-C16GL (**7**), it is thought that the introduction of fatty acids to all hydroxy groups increases the hydrophobic effect (solvophobic effect), which facilitates the formation of a three-dimensional supramolecular structure and improves gel hardness.

2.3. Field emission scanning electron microscopy (FE-SEM) observation

FE-SEM observation was performed on the xerogels derived from compounds **3**–**6** (C14GL–C22GL) among the 5 wt% gels described in section 2.2. Liquid paraffin #350 was removed to obtain xerogels by immersing each gel in acetone for one week, but the gels from C14GL (**3**) and C16GL (**4**) dissolved in acetone, so ethanol was used for deoiling for one week. FE-SEM observations were performed after the osmium coating of the obtained xerogels. **Figure 3** shows the FE-SEM images of various xerogels.

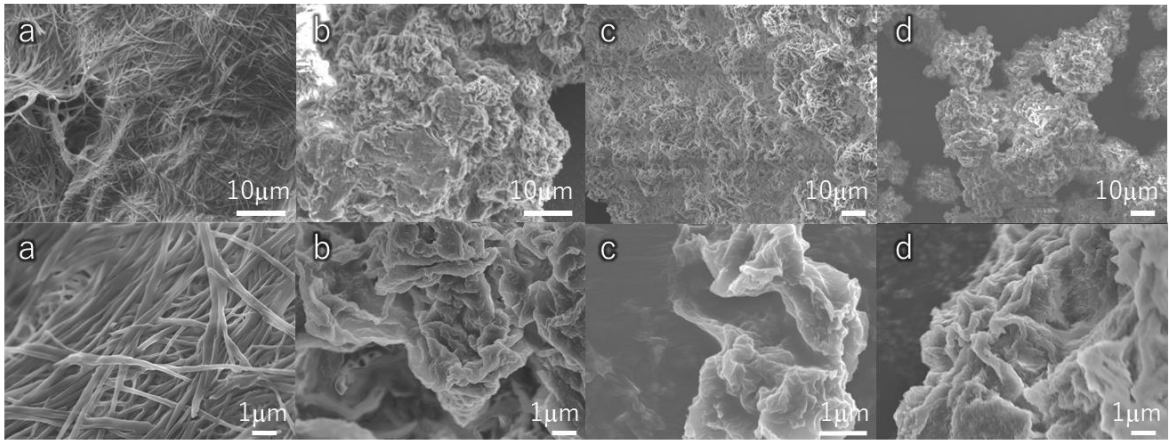

Figure 3. FE-SEM images of the xerogels from a 5 wt% gel of each sample in liquid paraffin #350. (a) C14GL (**3**), (b) C16GL (**4**), (c) C18GL (**5**), and (d) C22GL (**6**). The top and bottom photos show different magnification.

The C14GL (**3**) xerogel had a fiber structure with a diameter of 100–200 nm, while the other xerogels had a porous structure with plate-like crystals stacked three-dimensionally. Despite the same porous structure, C16GL (**4**), C18GL (**5**), and C22GL (**6**) exhibited different turbidity levels (**Table 1**). In other words, the size of the plate-like crystals themselves was comparable, although the overall structure was expected to be larger with longer fatty acids, which would increase aggregation. All of these compounds exhibited gelation ability, but the gelation mechanism differed depending on the length of the fatty acid, with some forming a fiber structure and others a porous structure.

2.4. Gelation test with various organic solvents using C18GL and comparison with the C16AG gel

The 5 wt% of C18GL (**5**), which exhibited the highest gelation ability as shown in **Table 1**, was used to examine the gelation ability in various oils (**Figure 4**).

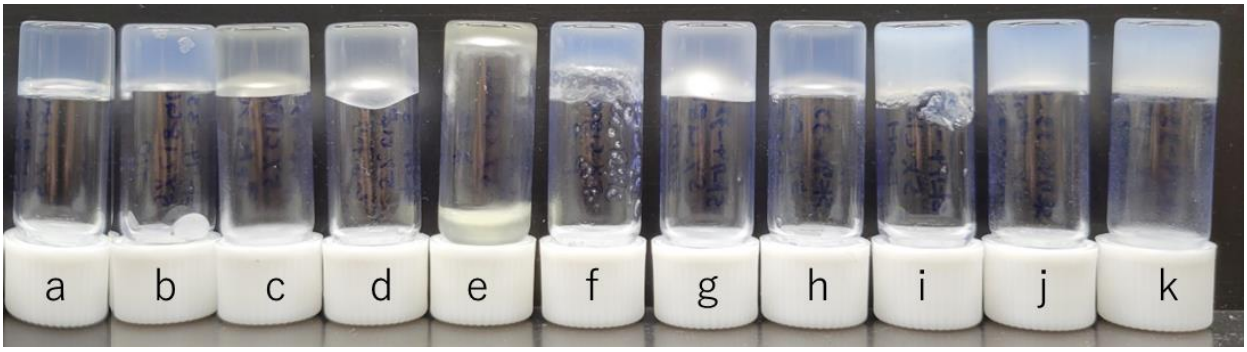

Figure 4. Actual photograph of the formed gels of each solvent; 5 wt% gel of C18GL (**5**) in various solvents and gel hardness (mN). (a) Liquid paraffin #350, 207 mN, (b) glyceryl tri(2-ethylhexanoate), 43 mN, (c) canola oil, 6 mN, (d) sunflower oil, 1 mN, (e) rice bran oil, flowed down, (f) 2-ethylhexyl palmitate, liquid separation, (g) diisostearyl malate, 5 mN, (h) cyclohexanol, 19 mN, (i) ethanol (99.5), 18 mN, (j) cyclopentasiloxane, 4 mN, and (k) dimethicone (6 mm^2/s), 89 mN.

The hydrocarbon oil, liquid paraffin #350 (a), produced the hardest gel. Glyceryl tri(2-ethylhexanoate) (b), an ester oil, formed a relatively hard gel, while canola oil (c), sunflower oil (d), and diisostearyl malate (g) formed soft gels. Rice bran oil (e) was too soft to gel. 2-Ethylhexyl palmitate (f) also formed an incomplete gel with liquid separation. Alcohols (h and i) and silicone oils (j and k) could gel. The FE-SEM study showed that C18GL (**5**) forms plate-like crystals building up to a porous structure. In contrast, C16AG (**8**) forms fiber structures. The inverted microscopy images showed fibers for C16AG (**8**), whereas C18GL (**5**) showed a mass of crystals (**Figure 5**).

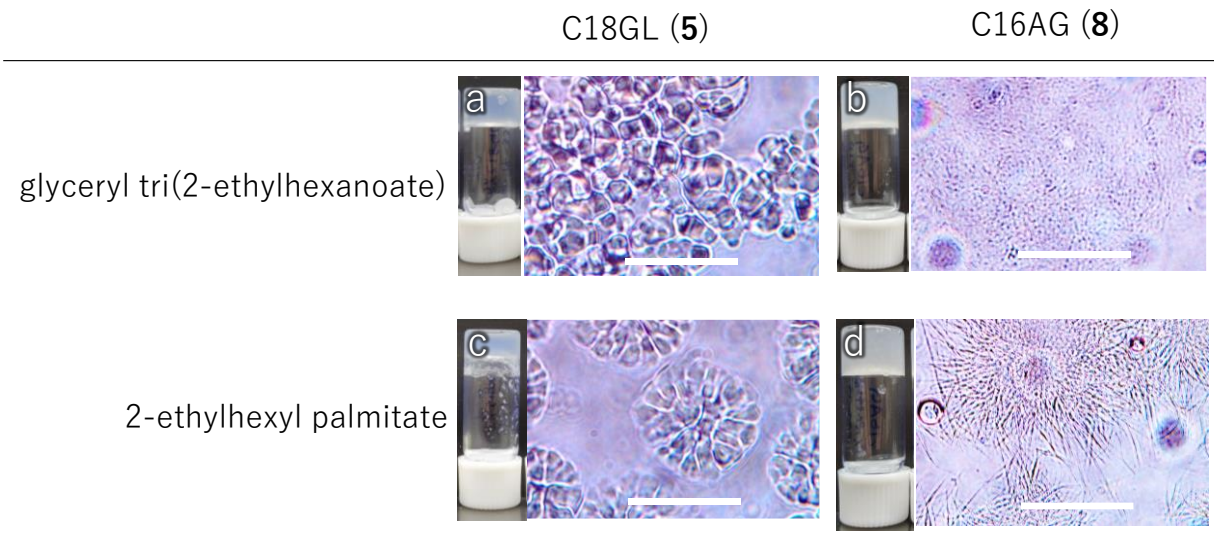

Figure 5. Appearance and differences between C18GL (**5**) and C16AG (**8**) gels. Actual photographs (left) and inverted microscope photographs (right). (a) 5 wt% of C18GL (**5**) in glyceryl tri(2-ethylhexanoate), (b) 1 wt% of C16AG (**8**) in glyceryl tri(2-ethylhexanoate), (c) 5 wt% of C18GL (**5**) in 2-ethylhexyl palmitate, and (d) 1 wt% of C16AG (**8**) in 2-ethylhexyl palmitate. Scale bars = 0.1 mm.

In addition, in 2-ethylhexyl palmitate, these crystalline masses gathered radially to form domains. We suggested that C16AG (**8**) gels by trapping oil between fibers, while C18GL (**5**) gels by trapping oil in a porous mass. This idea correlates well with the FE-SEM observations. In the mechanism of trapping oil between fibers, oil can be gelled with a small amount of gelator, while in the mechanism of trapping oil in a porous mass, oil cannot be gelled without increasing the concentration of gelator. Therefore, C16AG (**8**) can gel a variety of oils at 1 wt%, while C18GL (5) requires a concentration of 1 to 5 wt%.

2.5. X-ray diffraction (XRD) analysis

XRD analysis of compounds **2**–**6** was performed to determine the molecular arrangement. Clear diffraction peaks were obtained for compounds **2**–**5** (**Figure 6**), and these profiles suggested a

193 lamellar crystalline state (**Table 2**).

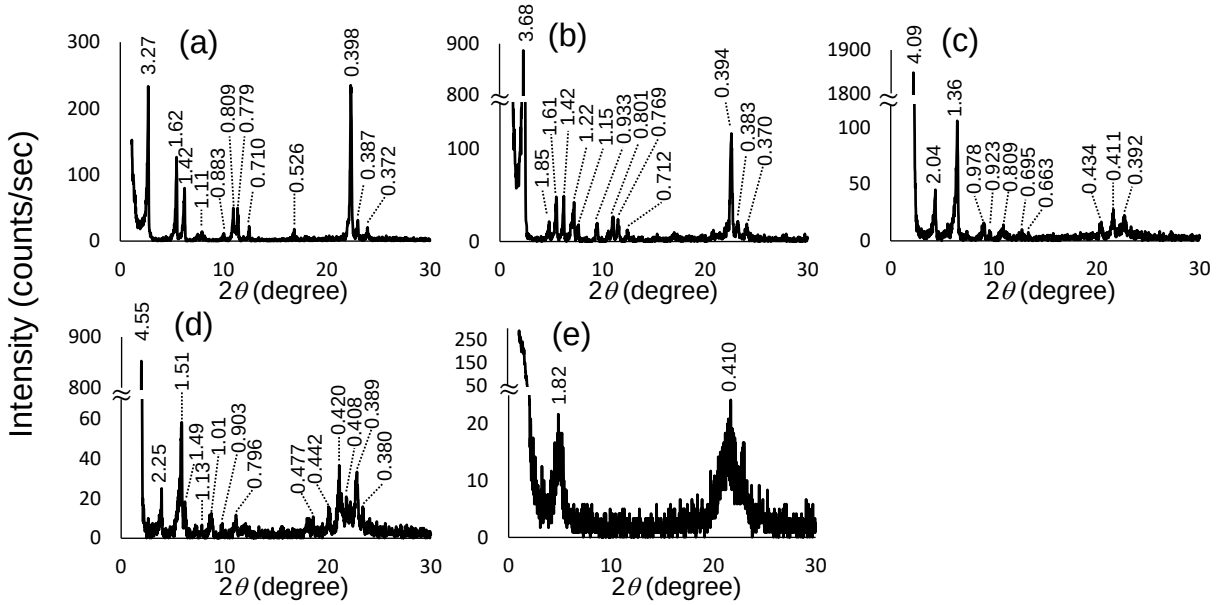

Figure 6. XRD patterns of (a) C12GL (**2**), (b) C14GL (**3**), (c) C16GL (**4**), (d) C18GL (**5**), and (e) C22GL (**6**)**.** The numbers indicate *d* spacings (nm).

194

Table 2. Distance (nm) and reflection attributions calculated from Bragg's law from the XRD pattern of neat powders for compounds **2**–**5**.

	Small-angle diffractions				
Compound	001	002	003	004	Wide-angle diffractions
C12GL (**2**)	3.27	1.62	1.11		0.526, 0.398, 0.387, 0.372
	1.42	0.710			
C14GL (**3**)	3.68	1.85	1.22	0.933	0.394, 0.383, 0.370
	1.61	0.801			
	1.42	0.712			
C16GL (**4**)	4.09	2.04	1.36		0.434, 0.411, 0.392
C18GL (**5**)	4.55	2.25	1.51	1.13	0.477, 0.442, 0.420, 0.408, 0.389, 0.380

195

196 Two lamellar structures were observed for C12GL (**2**) and three for C14GL (**3**). The ideal structure

with the lowest thermal energy, calculated using MOPAC in Chem3D software (PerkinElmer Software), was a compound in which the fatty acid chains attached to the 2- and 3-position hydroxy groups were in pairs, and the fatty acid chains attached to the 5- and 6-position hydroxy groups formed another pair, each extending in opposite directions. The α-position of the fatty acid chain attached to the 3- and 5-positions was twisted (Gauche), and the rest was in an all-*trans* structure. The calculated molecular lengths were 3.49 nm (C12GL (**2**)), 3.98 nm (C14GL (**3**)), 4.46 nm (C16GL (**4**)), and 4.94 nm (C18GL (**5**)). XRD results showed that for each compound, molecular lengths of 3.27 nm (C12GL (**2**)), 3.68 nm (C14GL (**3**)), 4.09 nm (C16GL (**4**)), and 4.55 nm (C18GL (**5**)) corresponded to lamellar structures. This is consistent with the lamellar structures obtained when they are aligned at angles of approximately 70°, 68°, 67°, and 67° to the horizontal plane, respectively. This lamellar structure became thicker as the number of fatty acid increased. In contrast, compound **6** (C22GL) showed only a broad peak. It is thought that the clear diffraction peak was not observed because C22GL (6) was purified by silica gel column chromatography and to powder, whereas the other compounds were powders obtained by crystallization. Each compound showed an average diffraction peak of 0.4 nm in wide-angle diffractions, corresponding to the average distance of 0.4 nm between two paired fatty acid chains, as known from calculations.

2.6. Emulsification tests

To verify the emulsification performance, we compared compounds **1**–**6** to Span 65 and 60 (sorbitan tristearate and monostearate, respectively, commercial emulsifiers), C16AG (**8**) (an existing organogelator), and dextrin palmitate (Rheopearl® KL2, a commercial organogelator). Each sample was accurately weighed using 2-mL screw-capped glass bottles, and liquid paraffin #350 was added to achieve a concentration of 1 wt% (approximately 500 mg in total). After adding 200 μL of water, the mixtures were heated on a hot plate at 100°C–150°C to dissolve the compounds and then

emulsified while hot using a hand sonic for 30 seconds. All samples were emulsified uniformly. The emulsions were left at room temperature for six days before observation (**Figure 7**).

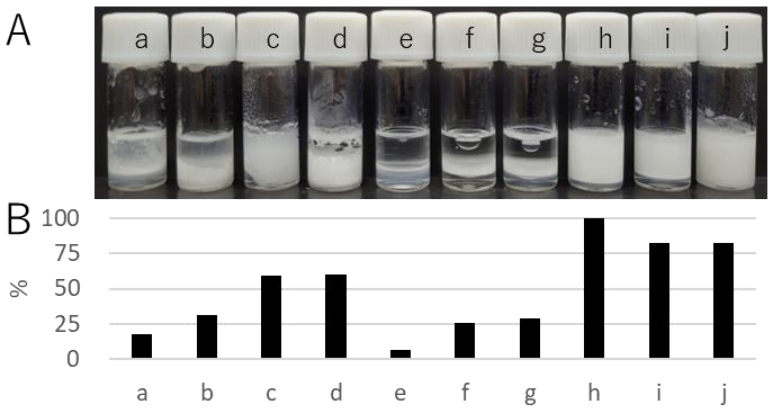

Figure 7. Photograph of the emulsification test and area of cream determined using image analysis. (A) Photograph of emulsion left at room temperature for six days after preparation. (B) Graphical representation of the relative area in % when the area of the cream in (h) C16GL (**4**) is 100, analyzed using image analysis software. (a) Span 65, (b) Span 60, (c) C16AG (**8**), (d) dextrin palmitate, (e) C10GL (**1**), (f) C12GL (**2**), (g) C14GL (**3**), (h) C16GL (**4**), (i) C18GL (**5**), and (j) C22GL (**6**).

The photograph was analyzed using image analysis software, ImageJ (National Institutes of Health, USA), to compare the cloudy emulsion (cream) area (**Figure S36** in the Supporting Information). C10GL (**1**), C12GL (**2**), and C14GL (**3**) exhibited poor emulsification stability and did not retain much cream. Similarly, the commercial emulsifiers Span 65 and 60 were also poorly stable. In contrast, the creams of C16GL (**4**), C18GL (**5**), and C22GL (**6**) were maintained much the same as they were prepared, indicating that they have high emulsification stability. The existing organogelators C16AG (**8**) and dextrin palmitate were shown to have inferior emulsion stability to C16GL (**4**), C18GL (**5**), and C22GL (**6**). C16AG (**8**), C16GL (**4**), and C18GL (**5**) could gel at 1 wt% in liquid paraffin #350, and all showed high emulsion stability. Dextrin palmitate and C22GL (**6**),

233 which cannot gel at 1 wt%, also exhibited high emulsion stability. This may be due to the thickening
234 effect. Comparing C16AG (**8**) and C16GL (**4**) protected by the same palmitic acid, C16AG (**8**) is
235 more effective as a gelator to create a harder gel, while C16GL (**4**) has better emulsion stability,
236 suggesting that the carbonyl group of the lactone ring may be effective in emulsion stability.
237
238 *2.7. Differential scanning calorimetry analysis*
239 Differential scanning calorimetry (DSC) measurements were performed to observe the thermal
240 behavior of each compound (**Figure 8**).

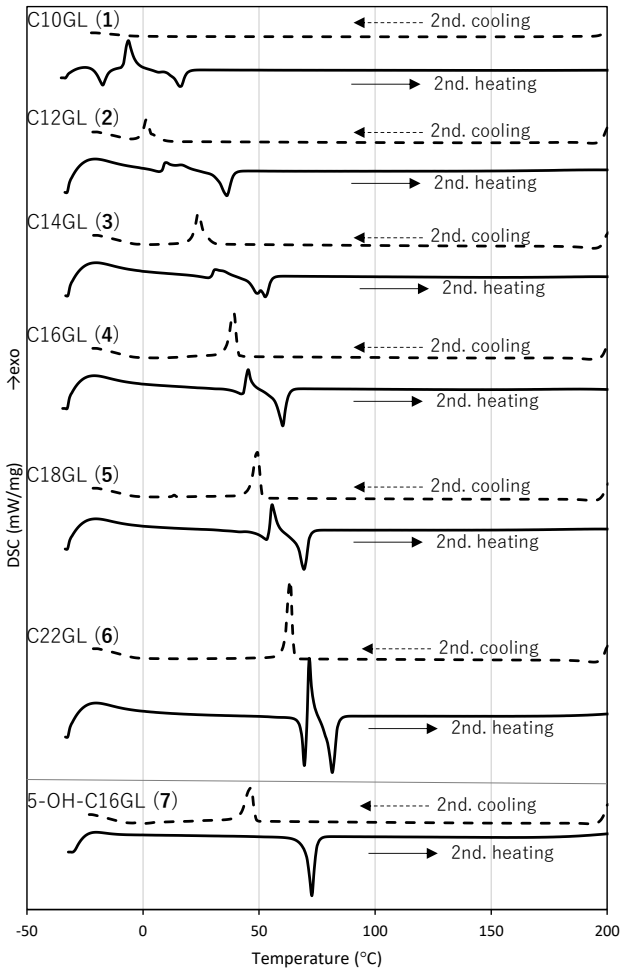

Figure 8. DSC charts of each compound using condition 1 (cooling and heating rate: 10°C /min). Cooling from 200°C to −30°C (dashed line). Heating from −30°C to 200°C (solid line). Owing to the low cooling capacity of the equipment, the cooling could not keep up at temperatures below −6.7°C, resulting in a reduced cooling rate and reaching only −21°C even though the final temperature was set at −30°C. About the dashed line of C10GL (**1**), the exothermic peak due to type I crystallization is not observed here. Before the second heating, we programmed to maintain the temperature at −30°C for 5 min, during which the actual temperature is cooled from −21°C to −30°C. The exothermic peak due to type I crystallization was observed during this step.

Each compound, except 5-OH-C16GL (**7**), exhibited an exothermic peak during cooling, due to polymorphic type I crystallization, and an endothermic peak during heating, which due to the melting of the type I crystals. Moreover, an exothermic peak during heating, possibly due to molecular realignment (type II crystallization), and a subsequent endothermic peak, due to the melting of type II crystals, were observed. The temperatures of the exothermic peak during cooling and the first endothermic peak during heating are very close, indicating they are the same phenomenon, capturing type I crystallization and melting. The exothermic peaks observed upon heating for these compounds indicate type II crystallization, where molecules transition to realigned second crystalline state. Since this type II crystallization during heating is accompanied by exothermicity and can be regarded as so-called cold crystallization, DSC measurements were performed at different heating rates (**Figure 9**). Compared to these compounds, 5-OH-C16GL (**7**) showed no crystal polymorphism. In other words, the introduction of fatty acids into all the hydroxy groups of 1,4-GL was essential to create the crystal polymorphism.

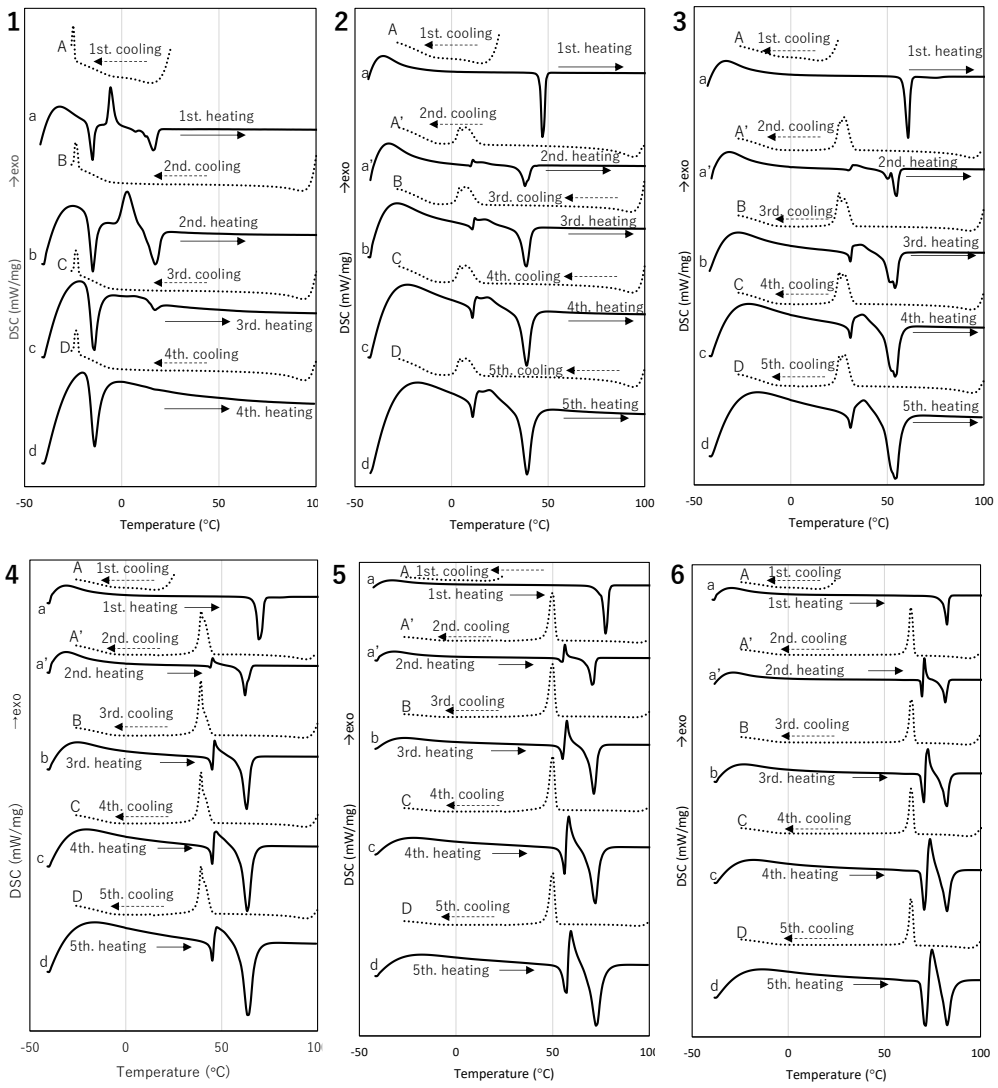

Figure 9. DSC charts with different heating rates using condition 2 (set cooling from 100°C to −40°C, except for the 1st cooling from 25°C to −40°C, and set heating from −40°C to 100°C). Each heating rate (solid line) is as follows: (a) and (a') 5°C/min, (b) 10°C/min, (c) 15°C/min, and (d) 20°C/min. All cooling rates are 10°C/min (dotted line). (1) C10GL (**1**), (2) C12GL (**2**), (3) C14GL (**3**), (4) C16GL (**4**), (5) C18GL (**5**), and (6) C22GL (**6**). Owing to the low cooling capacity of the equipment, the cooling rate could not keep up at temperatures below −6.7°C, resulting in a reduced cooling rate. Although the device was set to cool down to −40°C, it could only cool down to −26°C. By subsequently running a program that maintained the temperature at −40°C for 10 min, the initial temperature of the next heating measurement could be started at −40°C.

The peak temperature of the exothermic peak shifted to higher temperatures as the heating rate increased, indicating typical cold crystalline behavior. The crystallization energies of cold crystallization were calculated using **Equation 1** after creating a Kissinger plot with the Kissinger equation (**Figure S37** in the Supporting Information).[17]

$$\frac{d \ln (\lambda/T_p^{\,2})}{d\,(1/T_p)} = -\frac{E_a}{R}$$

Equation 1. T_p [K]: peak cold crystallization temperature on heating. λ [K min^{-1}]: temperature rate during heating. R [J K^{-1} mol^{-1}]: gas constant (8.314). E_a [kJ mol^{-1}]: crystallization energy of cold crystallization.

The crystallization energies were calculated to be 46, 217, 229, 528, 356, and 336 KJ mol^{-1} for compounds **1**–**6**, respectively. Crystalline samples with low crystallinity tend to have smaller crystallization energies. For example, C10GL (**1**) is crystalline because of the van der Waals forces from the fatty acid chain, but its short chain length and high degree of freedom result in lower crystallinity and smaller crystallization energy. C16GL (**4**) (palmitic acid with 16 carbons) has the highest crystallization energy, while compounds C18GL (**5**) and C22GL (**6**) with longer carbon chains exhibit decreasing crystallization energies. This suggests that 16-carbon palmitic acid has the highest intermolecular packing strength, whereas increasing carbon chain length makes packing more difficult, reducing the crystallinity and crystallization energy.

C10GL (**1**) is liquid at room temperature, exhibiting an endothermic peak due to type I crystallization in the first cooling. In the first heating, the observed sequence was melting of type I crystal, type II crystallization (cold crystallization), and type II crystal melting. As the heating rate increased, the temperature of the exothermic peak due to cold crystallization rose, overlapping with the endothermic peak from subsequent melting of crystals, causing the disappearance of distinct peaks at a heating rate of 20°C/min. The cold crystallization temperature is near 0°C, suggesting its potential application

as a heat storage material for ice melting.

C12GL (**2**), C14GL (**3**), C16GL (**4**), and C18GL (**5**) are solids crystallized in organic solvents. Therefore, only melting peak of these crystals was observed on the first heating. However, in DSC measurements with varying temperature increase, the melting points of its crystals in both type I and type II crystals were different from the melting point of the first crystal and were lower in temperature. Therefore, it was suggested that the crystals crystallized in the organic solvent were type III crystals. On the other hand, the melting point of C22GL (**6**) on the first heating was the same as that of the type II crystal. We speculate that this is because no special crystallization operation was performed after the column purification during the synthesis of C22GL (**6**), and therefore it did not become type III crystal. The lamellar structure observed in the XRD analysis was found to be derived from type III crystals. We also speculate that C22GL (**6**) was a type II crystal, which caused the broad XRD pattern. Thus, the C-GL series, in which fatty acids were introduced into all hydroxy groups, was found to have type I, type II, and type III crystal polymorphism.

2.8. Fourier transform infrared spectroscopy analysis

To analyze each crystal state of the crystal polymorphism of C18GL (**5**) in detail at the molecular level, Fourier transform infrared spectroscopy (FT-IR) was used to measure type I, type II, and type III crystals and a solution melted at 100°C (**Figure 10**, see also **Figure S38** in the Supporting Information). Characteristic peaks were observed for the carbonyl ester stretching peaks in each crystal form (**Table 3**). The wavenumber of the aliphatic carbonyl stretching peak decreased as the crystal form progressed from type I to II and III. Type I had a peak at 1748–1749 cm^{-1}, the same as the liquid form, and no intermolecular hydrogen bonding. In types II and III, the wavenumber of the stretching peaks gradually decreased to 1744 cm^{-1} and 1741 cm^{-1}, respectively. In other words, it is believed that the intermolecular hydrogen bonding gradually limits the carbonyl ester stretching. On

the other hand, γ-lactone has two carbonyl stretching peaks at 1820 cm^{-1} and 1809 cm^{-1} in the liquid state. Type I has a peak at 1810 cm^{-1} and no intermolecular hydrogen bonding. Compared to type I, types II and III have peaks 1820 cm^{-1} and 1803 cm^{-1}. Peak 1820 cm^{-1} is also in the liquid and is not used for intermolecular hydrogen bonding, while peak 1803 cm^{-1} appears to be used for intermolecular hydrogen bonding. Thus, as the crystal polymorphism progresses from I to II and III, the aliphatic and γ-lactone carbonyl groups become less stretched and intermolecular hydrogen bonds are formed. The Type I crystals have no intermolecular hydrogen bonds and melt at low temperatures, and the formation of intermolecular hydrogen bonds by the carbonyl groups of γ-lactone and fatty acids is thought to change the crystal form to type II and type III and increase the melting point.

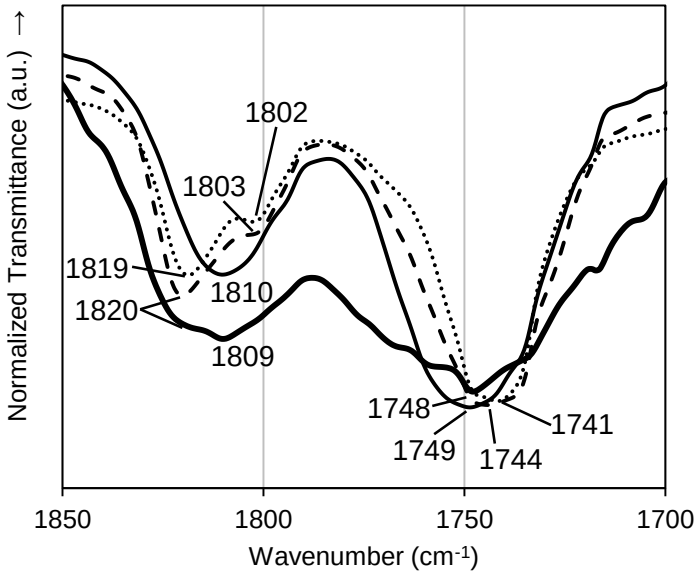

Figure 10. FT-IR spectra of type I, type II, and type III crystals and solution (100°C) of C18GL (**5**). The carbonyl [ν(-C=O)] ester stretching regions from 1700–1850 cm^{-1} are shown. 1750–1820 cm^{-1} are stretching regions of lactone and 1735–1750 cm^{-1} are stretching regions of aliphatic ester. Type I crystal (solid line). Type II crystal (dashed line). Type III crystal (dotted line). Solution at 100°C (bold line).

310

Table 3. Wavenumber (cm^{-1}) of FT-IR spectra of carbonyl ester stretching regions (lactone and aliphatic ester stretching regions) for each type of crystal and solution (100°C).

Crystal type	Lactone (cm^{-1})			Aliphatic ester (cm^{-1})		
Solution	1820	1809		1748		
Type I		1810		1749		
Type II	1820		1803		1744	
Type III	1819		1802			1741

311

312 **3. Conclusions**

313 We focused on 1,5-GL as a sugar that does not require protection at the anomeric position and

synthesized compounds protected with various linear saturated fatty acids (C-GL series) in only one step for developing novel organogelators. In all cases, the compounds were obtained in which the six-membered ring structure was changed to a five-membered ring structure (1,4-GL). We believe this is because the five-membered ring is thermodynamically more stable when the fatty acid is introduced into the 6-position hydroxy group of 1,5-GL. The C-GL series synthesized here inferior gelation ability compared to C16AG, an existing gelator with six-membered ring structure. The first reason for this is thought to be weakening of the intermolecular packing force due to the increased degrees of freedom of the carbons at 5- and 6-positions of the five-membered ring. Furthermore, this may be reflected in the xerogel structure, as revealed by FE-SEM observations. Compounds with molecular chains longer than 16 carbons form a porous structure with irregular plate-like crystals rather than the fiber structure typical of LMG. However, XRD measurements of C12GL to C18GL showed a lamellar structure with regularly arranged molecules. The existing LMG, C16AG, has a lamellar structure, forming a fiber structure with a diameter of 100–200 nm. When the lamellar structure extends in one direction, fibers are formed, but when it extends in multiple directions, plate-like crystals are formed. We conclude that the gelation mechanism of C16GL to C22GL is the confinement of oil in the porous structure created by the plate-like crystals, which results in the loss of fluidity and gelation. Compared to fibers, porous structures require higher concentrations of a gelator to gel the same volume of oil. This may be the second reason why the gelation ability of the C-GL series synthesized in this study is inferior to that of C16AG, an existing gelator.

In addition to being used as an organogelator, the C-GL series was also intended to be used as a new emulsifier. As expected, C16GL to C22GL were found to have very high emulsification stability. They had better stability than the existing organogelators C16AG and dextrin palmitate. While these existing organogelators stabilize the emulsified state by increasing the oil's viscosity, we believe that the C-GL series stabilizes the emulsified state by increasing the oil's viscosity moreover some

interaction with water. In other words, we speculate that the carbonyl oxygen atom at the γ-lactone, which is characteristic of C-GL series, improves the affinity with water and stabilizes the emulsified state. Among these, C16GL and C18GL were found to gelate oil at relatively low concentrations and high emulsion stability and are expected to be applied in the cosmetics and painting fields.

DSC measurements revealed that the C-GL series except for 5-OH-C16GL (**7**) has crystal polymorphism. There were three types of crystals: type I crystals precipitated by rapid cooling, type II crystals precipitated by heating, and type III crystals precipitated by using organic solvents. Among the C-GL series, C10GL is liquid at room temperature, but when it was solidified by rapid cooling and then slowly heated, an exothermic peak, type II crystallization peak, was observed near 0°C. This is cold crystallization due to C10GL's heat storage properties, which is expected to have an ice-melting effect. In the C-GL series, the exothermic temperature due to cold crystallization (type II crystallization) varies depending on the length of the fatty acid. When used as a heat storage material, the exothermic temperature can be controlled by simply changing the length of the fatty acid, and we speculate that it can be used as a heat storage material that suits the purpose. Furthermore, FT-IR measurements of each crystal polymorph indicate that intermolecular hydrogen bonds are formed by carbonyl groups as the crystal polymorph shifts from I to II and III. This is the reason for the increase in melting point. Furthermore, correlation with XRD measurements revealed that a lamellar structure is formed in type III crystals. Since there is no crystal polymorphism in 5-OH-C16GL (**7**), fatty acid binding to all hydroxy groups of 1,4-GL is required to create the crystal polymorphism.

Thus, a novel C-GL series was synthesized, and their physical properties were elucidated in detail. In the future, we plan to apply the physical properties of these compounds for practical applications.

Supporting Information: Materials and methods (general methods, preparation of per-*O*-linear saturated fatty acyl-protected D-glucono-1,4-lactone, gelation evaluation, hardness measurements,

turbidity measurements, FM-SEM observation, inverted microscope observation, XRD analysis, emulsification test, DSC analysis, and FT-IR analysis) of compounds **1**–**7**. ^{1}H, ^{1}H–^{1}H COSY, ^{13}C, HSQC, and HMBC-NMR charts of compounds **1**–**7**. How to determine the area of cream. Kissinger plots of compounds **1**–**6**. FT-IR spectra of type I, type II, and type III crystals and solution (at 100°C) (PDF).

Funding: This work was supported by the JSPS KAKENHI, Grant Number JP21K05418.

Acknowledgments: This research was conducted using NMR and MS equipment owned by the Advanced Analysis Center, National Agriculture and Food Research Organization (NARO), JP. We thank H. Ono (Advanced Analysis Center, NARO, JP) and his staff for the NMR and matrix-assisted laser desorption ionization–time of flight mass spectrometry measurements.

Conflicts of Interest: The author declares no conflicts of interest.

References

1. Tyagi, R.; Singh, K.; Srivastava, N.; Sagar, R. Recent Advances in Carbohydrate-Based Gelators. *Mater. Adv.* **2023,** *4* (18), 3929-3950. DOI: 10.1039/d3ma00321c
2. Cheuk, S.; Stevens, E. D.; Wang, G. Synthesis and Structural Analysis of a Series of D-Glucose Derivatives as Low Molecular Weight Gelators. *Carbohydr. Res.* **2009,** *344* (4), 417-425. DOI: 10.1016/j.carres.2008.12.006
3. Wang, G. J.; Cheuk, S.; Yang, H.; Goyal, N.; Reddy, P. V. N.; Hopkinson, B. Synthesis and Characterization of Monosaccharide-Derived Carbamates as Low-Molecular-Weight Gelators. *Langmuir* **2009,** *25* (15), 8696-8705. DOI: 10.1021/la804337g
4. Soundarajan, K.; Rajasekar, M.; Das, T. M. Self-Assembly of Sugar Based Glyco-Lipids: Gelation Studies of Partially Protected D-Glucose Derivatives. *Mater. Sci. Eng. C Mater. Biol. Appl.* **2018,** *93*, 776-781. DOI: 10.1016/j.msec.2018.08.038
5. Ludwig, A. D.; Saint-Jalmes, A.; Mériadec, C.; Artzner, F.; Tasseau, O.; Berrée, F.; Lemiègre, L. Boron Effect on Sugar-Based Organogelators. *Chem. - Eur. J.* **2020,** *26* (61), 13927-13934. DOI: 10.1002/chem.202001970
6. Ono, F.; Ichimaru, K.; Hirata, O.; Shinkai, S.; Watanabe, H. Universal Glucose-Based Low-Molecular-Weight Gelators for Both Organic and Aqueous Solvents. *Chem. Lett.* **2019,** *49* (2), 156-159. DOI: 10.1246/cl.190769

7. Guan, X. D.; Fan, K. Q.; Gao, T. Y.; Ma, A. P.; Zhang, B.; Song, J. A Novel Multi-Stimuli Responsive Gelator Based on D-Gluconic Acetal and Its Potential Applications. *Chem. Commun.* **2016,** *52* (5), 962-965. DOI: 10.1039/c5cc08615a
8. Chen, S. P.; Zhang, B. H.; Zhang, N. X.; Ge, F. S.; Zhang, B.; Wang, X. J.; Song, J. Development of Self-Healing D-Gluconic Acetal-Based Supramolecular Ionogels for Potential Use as Smart Quasisolid Electrochemical Materials. *ACS Appl. Mater. Interfaces* **2018,** *10* (6), 5871-5879. DOI: 10.1021/acsami.7617099
9. Fan, K.; Wang, X.; Wang, X.; Yang, H.; Han, G.; Zhou, L.; Fang, S. One-Step-Synthesized D-Gluconic Acetal-Based Supramolecular Organogelators with Effective Phase-Selective Gelation. *RSC Adv.* **2020,** *10* (61), 37080-37085. DOI: 10.1039/d0ra07658a
10. Kajiki, T.; Komba, S. Development of Novel Low-Molecular-Mass Oil-Gelling Agents: Synthesis and Physical Properties of 1,5-Anhydro-D-Glucitol and 1,5-Anhydro-D-Mannitol Protected with Saturated Linear Fatty Acids. *J. Appl. Glycosci.* **2019,** *66* (3), 103-112. DOI: 10.5458/jag.jag.JAG-2019_0011
11. Kajiki, T.; Komba, S.; Iwaura, R. Supramolecular Organogelation Directed by Weak Noncovalent Interactions in Palmitoylated 1,5-Anhydro-D-Glucitol Derivatives. *ChemPlusChem* **2020,** *85* (4), 701-710. DOI: 10.1002/cplu.202000147
12. Iwaura, R.; Komba, S.; Kajiki, T. Supramolecular Fibrous Gels with Helical Pitch Tunable by Polarity of Alcohol Solvents. *Soft Matter* **2021,** *17*, 1773-1778. DOI: 10.1039/d0sm02136a
13. Komba, S.; Iwaura, R. High-Temperature Solvent-Free Synthesis of Low-Molecular-Weight Organogelators Consisting of Starch-Derived 1,5-Anhydro-D-Glucitol Coupled with Fatty Acids. *RSC Adv.* **2023,** *13* (14), 9316-9321. DOI: 10.1039/d3ra01328f
14. Komba, S.; Iwaura, R. Development of Low-Molecular-Mass Organogelators: Synthesis and Physical Properties of N-Linear Saturated Fatty Acyl-Gabas and Their Ester Derivatives. *Acs Omega* **2021,** *6* (32), 20912-20923. DOI: 10.1021/acsomega.1c02240
15. Pocalyko, D. J.; Carchi, A. J.; Harirchian, B. Selective Monoacylation of Aldonolactones by Lipase-Catalyzed Transesterification. *J. Carbohydr. Chem.* **1995,** *14* (2), 265-270. DOI: 10.1080/07328309508002069
16. Kwoh, D.; Pocalyko, D. J.; Carchi, A. J.; Harirchian, B.; Hargiss, L. O.; Wong, T. C. Regioselective Synthesis and Characterization of 6-O-Alkanoylgluconolactones. *Carbohydr. Res.* **1995,** *274*, 111-121. DOI: 10.1016/0008-6215(95)00074-4
17. Kissinger, H. E. Reaction Kinetics in Differential Thermal Analysis. *Anal. Chem.* **1957,** *29* (11), 1702-1706. DOI: 10.1021/ac60131a045